A study of the interaction between coolant jet nozzle flow and the airflow around a grinding wheel in cylindrical grinding

Originally published in:
Procedia CIRP 58, https://doi.org/10.1016/j.procir.2017.03.261

Available online at www.sciencedirect.com

ScienceDirect

Procedia CIRP 58 (2017) 517 – 522

www.elsevier.com/locate/procedia

16th CIRP Conference on Modelling of Machining Operations

A study of the interaction between coolant jet nozzle flow and the airflow around a grinding wheel in cylindrical grinding

Christoph Baumgart[a]*, Julian J. Radziwill[a], Friedrich Kuster[a], Konrad Wegener[a]

[a]*Institute of Machine Tools and Manufacturing (IWF), ETH Zürich, 8092 Zürich, Switzerland*

* Corresponding author. Tel.: +41 44 632 8981; Fax: +41 44 632 1125. *E-mail address:*baumgart@iwf.mavt.ethz.ch

Abstract

A grinding wheel rotating at high circumferential speed induces a boundary-layer airflow which possibly can detain the coolant from submerging into the grinding zone, in order to prevent thermal damage. To study the profile of the airflow, general laws of fluid dynamics are applied and the analytical results compared with results from CFD simulations. These are used to investigate the interaction of the coolant with the grinding wheel under the influence of the airflow with different coolant nozzle types and parameters. For validation high speed imaging is employed. The conclusions may help for a general understanding of the interaction between wheel-airflow-coolant.

Peer-review under responsibility of the scientific committee of The 16th CIRP Conference on Modelling of Machining Operations

Keywords: Grinding; Simulation; Cooling Fluid; Airflow

1. Introduction

A suitable coolant delivery remains crucial in conventional and energy intense grinding processes. Malkin and Anderson described the high thermal flux into the workpiece by plowing and sliding of the grinding grains and possible thermal damage due to high surface temperatures [1,2]. However an inefficient usage of coolant can contribute largely to the total energy balance of the machine and thus the production costs to a remarkable share [3]. The flood cooling method, which is still widely used in industry, generally delivers huge amounts of coolant at low pressures and undefined direction onto the grinding wheel and grinding zone, where typically a large amount of the fluid is neither used for cooling nor lubrication in the grinding zone. An experimental investigation counted only 4-30% of the coolant flow passing through the grinding zone [4]. The velocity ratio between coolant and tangential speed of the grinding wheel, the alignment of the coolant nozzles as well as their shape have been identified as the most significant factors for an efficient coolant delivery [5,6]. Much research has been done on jet nozzles to reduce the amount of fluid required and thus significantly lower the energy consumption by evaluating different nozzle designs in flat [7] as well as cylindrical grinding [8,9], where round nozzles allowed substantial lower coolant volume flows. Research and experience in industry clearly show that the coolant can be inhibited from entering into the grinding zone by the air boundary layer around the rotating grinding wheel. This phenomenon is also known as the air barrier [9]. Thus for the optimal design of fluid supply intense knowledge about the airflow is essential.

In literature many investigations about the boundary layer flow of grinding wheels can be found, most of them dealing with face grinding. Starting with schlieren imaging of the airflow [10], measurements with intrusive methods like hot-wire-anemometers [11] and the non-intrusive laser Doppler anemometry [12] have been used to investigate the flow conditions for cylindrical grinding wheels in radial and axial dimensions. Different velocity

Peer-review under responsibility of the scientific committee of The 16th CIRP Conference on Modelling of Machining Operations
doi:10.1016/j.procir.2017.03.261

distributions in outer and central regions of the grinding wheel surface have been detected. In recent years computational fluid dynamics (CFD) became a powerful and feasible tool for investigating various parameters including the influence of the surface roughness, porosity of the grinding wheel and the effect of air scrapers on the wheel boundary flow [13,14].

This work aims to contribute for the understanding of the interaction of the coolant jet of different nozzle types with the grinding wheel considering the airflow. As stated in [15] the Rouse shape nozzle is considered in literature as being optimal concerning jet flow quality in terms of coherence and disturbances. But the distribution of the coolant across the width of the grinding wheel (axial direction) for wider wheels as well as the interaction with the airflow is often neglected. First the general velocity distribution for a cylindrical shaped grinding wheel is shown. In a second part the interaction between coolant jets and the airflow field is investigated whereas the effect on the grinding process of the nozzles is known [8,9]. Full 3D-CFD simulations were performed and compared to high-speed images of an experimental set-up.

2. Analytical Equations

A complete analytical solution of the airflow around a rotating grinding wheel does not exist, but general remarks can be given. The grinding wheel is modeled by a rotating disk with basically two outer flow regions, the flow over the faces and the lateral flow respectively. When considering the porosity of a grinding wheel an inner flow through the tool can influence both regions.

Air as a viscous medium sticks on the walls of the rotating disk and is accelerated up to the surface velocity at the wall. The radial velocity profile away from the wall is defined by the inner friction. For several boundary layer flows exist empirical values related by the Reynolds number of the flow. For example the flow profile on the side faces can be modeled as a rotating disk, where an analytical solution is given by Schlichting [16]. Driven by velocity gradients the air is flowing to the lateral area of the wheel. To solve the Navier-Stokes equations analytically for the circumferential area of a disk, a general solution cannot be presented. Simplifying these equations leads to a velocity profile, which does not match with measurements or simulations as a result of the side and radial flow from the inner wheel. Analyzing various velocity profiles from simulations and measurements a function (1) is found describing the velocity profile in peripheral direction in the middle of the disc, where the peripheral velocity $u(r)$ reaches its maximum, by construction of the known dependencies:

$$u(r) = \frac{c_1}{\left(\left(r + \frac{c_4}{1000}\right)c_2\right)^{c_3}} \qquad (1)$$

with r as the radius, greater as the wheel Radius R. The constants c_1 *to* c_4 are depending on the viscosity, wall velocity, surface topology and geometrical parameters. Figure 1 shows a fit of the trial function with a measured velocity profile from [12] and with a simulation of the airflow of a rotating grinding wheel in the center of the peripheral areas (boundary conditions explained in the next chapter, no workpiece).

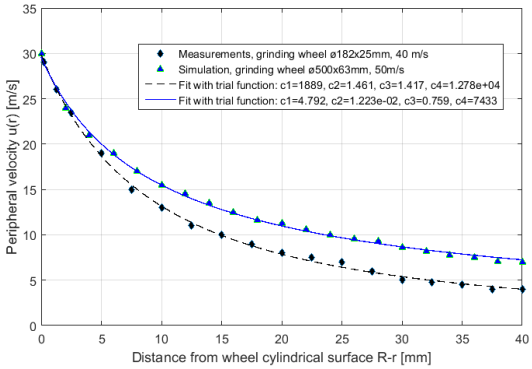

Fig. 1. Measured airflow velocities for two different grinding wheels for measurement and simulation each compared with the trial function.

Setting the assumptions static, rotational symmetric, uncompressible, no volume forces, very long cylinder and the boundary condition no airflow through the wall of the disc, the continuity results in $u_r=0$. The simplified Navier-Stokes equations in r-direction are

$$-\frac{u_\phi^2}{r}\rho = -\frac{\partial p}{\partial r} \qquad (2)$$

as considering $u_\varphi(r=R)=\omega R$ and $u_\varphi(r=\infty)=0$, leads to the simplified Navier-Stokes equations in φ-direction:

$$u_\phi(r) = \frac{\omega R^2}{r} \qquad (3)$$

Combining equation 2 and 3 and assume $p(r=\infty)=p_\infty$, the resulting pressure profile $p(r)$ in radial direction in cylinder coordinates is

$$p(r) = p_\infty - \frac{1}{2}\frac{v_c^2 \cdot R^2}{r^2}\cdot\rho \qquad (4)$$

and enables to make plausible conclusions, with v_c the tangential velocity at the wheel surface, p_∞ the ambient pressure and ρ the density of the air. The pressure close to the surface is lower than the pressure in the distant ambient and increases square hyperbolic in radial direction until the second term disappears in infinity. This pressure profile does not match with measurements of commonly used grinding wheels due to the wide cylinder approach. Nevertheless, the principle of pressure decrease appears in both situations. The lower pressure sucks the air from the side areas towards the circumferential area center, which is shown in more detail in the following simulations.

3. Numerical Analysis and Validation

3.1. Boundary conditions and flow field

In this section a full 3D steady state fluid simulation using ANSYS CFX 17.0 is presented. Following a mesh study a cylindrical ambient is chosen. In the set up a gap between the grinding wheel (solid, rotating) and the workpiece (solid, non-rotating) is left. The coolant is modeled using water data, as viscosity and density are measured the same as water. For all walls inflation layers are applied on the mesh in order to calculate wall functions resolving the boundary layer accurately. Residuals below 10^{-4} for convergence of momentum and pressure are achieved. Detailed information is given in Table 1.

Table 1. Experimental conditions

Grinding Wheel (Ø 500 x 63)		54A 120 H15 VPMF604W	
Cutting speed	v_c	50	[m/s]
Rotational speed	n_w	1910	[1/min]
Gap Grinding Wheel-Workpiece		10	[µm]
Workpiece (Ø 60 x 60)		90MnCrV8, 62 HRC	
Coolant		Water emulsion (4% in water)	
Volume Flow	Q	6-30	[l/min]
Flow rate per width	q	0.1-0.5	[l/(min mm)]
Nozzles		*Position*	
Height over grinding zone	H_{Noz}	70	[mm]
Orientation		Tangential into grinding arc	
		Round Jet Nozzle	
Inner Diameter	D_{in}	1.5	[mm]
Channels	N	4	[-]
		Flat Nozzle	
Width	B_{flat}	63	[mm]
Opening thickness	D_{flat}	1.5	[mm]
Ambient (Ø 1000 x 250)		Opening	1 [atm]
Physical properties		Air & Water, 25°C constant temperature	
Turbulence Model		Shear Stress Transport	
Surface Tension Coeff.	γ	0.072	[N/m]
Drag Coefficient	c_D	0.44	[-]
Buoyancy model activated, isothermal, no heat model applied			

ANSYS CFX 17.0

Figure 2 shows the velocity vectors on the grinding wheel. As assumed the airflow on the wheel faces is sucked into the center line from the lateral area and due to centrifugal forces directed away from the wheel (radial velocity > 0). It can be noted that for wider wheels this inhomogeneity becomes more important.

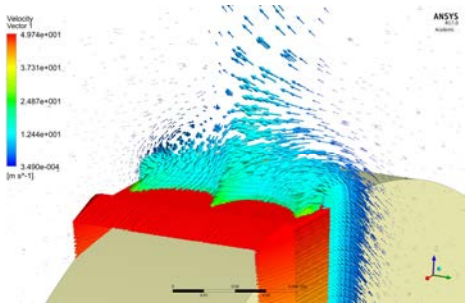

Fig. 2. Velocity vectors for a Ø 500 x 63mm grinding wheel at v_c = 50m/s.

In Figure 3 isosurfaces of the air velocity for the grinding wheel are shown. On the left figure it can be seen that in the middle, as well as close to the sides maxima exist. On the right figure the influence of a workpiece onto the airflow is shown.

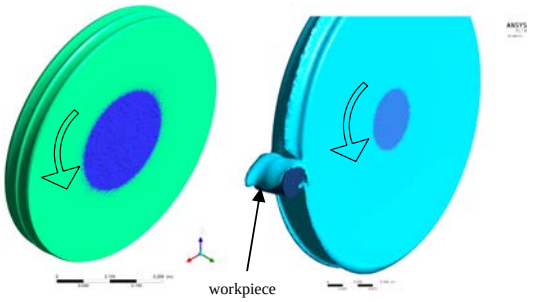

Fig. 3. Velocity Isosurfaces for a Ø 500 x 63mm grinding wheel at v_c = 50m/s. Left: v_{air} = 25m/s. Right: v_{air} = 10 m/s with workpiece.

Li and Han [17] proposed a boundary line for a suitable direction of the cooling flow in flat grinding. If the coolant is directed in an angle within the boundary line and the grinding wheel, the peripheral airflow of the

grinding wheel supports the coolant reaching the grinding zone. It is specified by velocity vectors without component pointing into the grinding gap. A similar pattern is observed in cylindrical grinding as shown in Figure 4. Furthermore the air flows around the workpiece and is driven back to the grinding wheel by a lower pressure field behind the workpiece, which works similar as an air scraper and has to be treated in respect to the workpiece size as shown in Figure 3, right side.

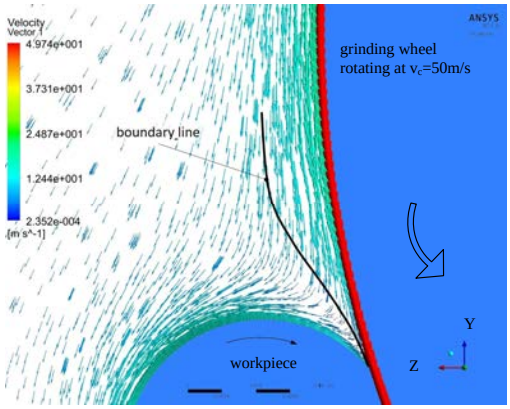

Fig. 4. Boundary line as specified in [17] for cylindrical grinding, Ø 500 x 63mm grinding wheel and Ø 60 x 60mm workpiece yz-plane.

3.2. Comparison with high-speed imaging

High speed (HS) imaging is a versatile tool to qualitatively determine the interaction of grinding wheel airflow and coolant jet. The adherence of the coolant to the grinding wheel, which is necessary to reach the grinding zone and lubricate the cutting process, can be visualized as shown in Figure 5. In this case the exit velocity of the coolant is too low (about 20% of the tangential velocity of the grinding wheel) and the jet is deflected from the grinding wheel. The flow regime of the jet itself is strongly non-linear and interacts with the air flow around the grinding wheel. It varies from a coherent jet to a break-up into a spray. HS imaging is a helpful tool to validate simulations for the used flow model. In Figure 6 the flow direction of the coolant is changed into the centerline and away from the lateral face of the grinding wheel by the radial airflow from the wheel, as it is described in the former sections. The coolant (red) seems to disappear below but instead the volume fraction becomes lower and thus is not shown.

Also a characteristic of these steady state simulations can be observed. The blue and red jet streams in the simulation plots in Figures 3 and 5-8 are the isosurfaces for a specified coolant volume fraction of about 0.02. This value appears quite low, but comparing to the high speed camera images give rather a probability distribution of coolant in a volume and thus also the mixing with air, which has negative influence on the cooling in the grinding arc. The breakup in droplets or sprays cannot be resolved by steady state simulation and turbulence models and appears in rather wide distribution and dilution of the coolant stream.

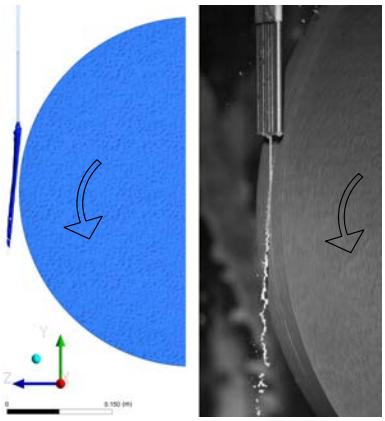

Fig. 5. One round nozzle, exit velocity about 20% of v_c = 50m/s a) simulation (coolant volume fraction 2%), b) HS-imaging

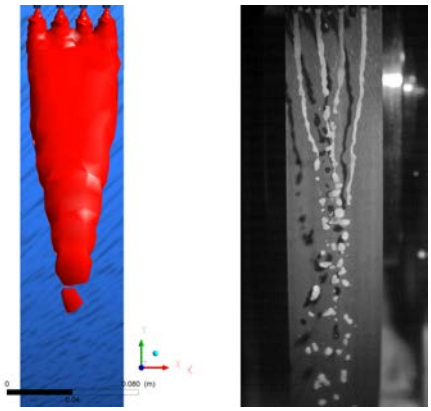

Fig. 6. Four round nozzles, exit velocity about 20% of v_c = 50m/s a) simulation (coolant volume fraction 0.5%), b) HS-imaging.

3.3. Interaction of airflow with coolant jet

Figures 7 and 8 are showing the isosurfaces of the coolant volume fraction at 2% for the two investigated nozzle types. The round nozzles apparently deliver the coolant much more precise into the grinding zone with less flooding of coolant over the workpiece. The airflow seems to have much higher influence on the coolant flow out of the flat nozzle type, because contrary to the needle nozzles it is hindered by the flat nozzles to flow out in radial direction.

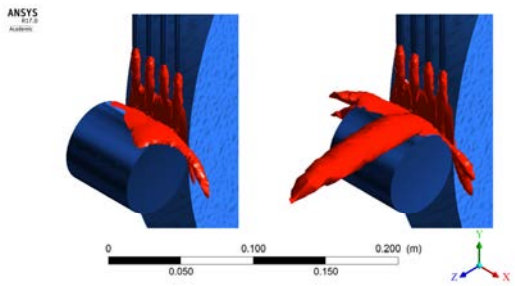

Fig. 7. Grinding wheel with v_c = 50m/s and a Ø60mm workpiece; coolant delivery by 4 round nozzles with left 6l/min and right 18l/min.

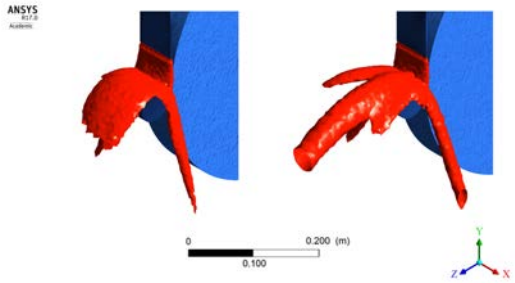

Fig. 8. Grinding wheel with v_c = 50m/s and a Ø60mm workpiece; coolant delivery by flat nozzles with left 18l/min and right 30l/min.

3.4. Results

The results of the simulations can help to understand the results of the grinding studies presented in [8,9], where different nozzle types are compared by their coolant volume flow rates for achieving the same surface properties on the workpiece. In this investigation the coolant volume flows of 6l/min for the round nozzles and 30l/min for the flat nozzle respectively are necessary to obtain the same roughness distributions. The following investigations refer to the properties on the grinding wheel in the grinding zone.

Figure 9 shows the volume fractions of the coolant in the grinding zone at the wheel side. Whereas the four single round nozzles could fill the grinding zone evenly with a total volume flow of 6l/min, which is equivalent to a specific volume flow of 0.1l/(min mm) over the grinding wheel, the flat nozzle fails to do so even using at least three times as much coolant. Even a small volume fraction of air can impair the cooling conditions essentially. The reason clearly is found in the much higher (18.5m/s vs. 4.5m/s) exit velocity of the coolant due much lower exit area (7mm^2 vs. 95mm^2) of the flat nozzle, that can break through the momentum of the airflow.

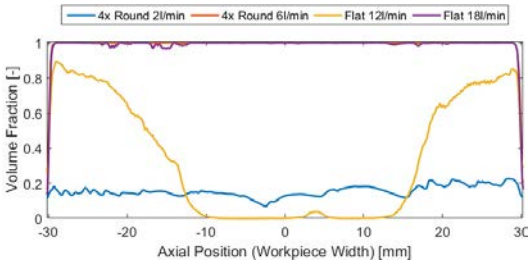

Fig. 9. Volume fraction of coolant in the grinding contact zone over workpiece width for different nozzles and flow rates.

Consistent with the study of the velocity profile of the airflow (shown in Figure 2) and theoretical consideration in the previous chapter, Figure 9 indicates the non-uniform impact of the airflow on the coolant jet. If the momentum of the coolant is too low the coolant is prevented from entering the grinding zone. Using the flat nozzle this can be provoked by lowering the coolant flow. If a volume flow of 12l/min coolant is supplied only the outsides of the grinding zone are flooded with coolant, while the middle section stays dry due to higher momentum of the airflow. As a result thermal damage as a result of undercooling can occur in the middle section of the workpiece. In industry often higher coolant flow rates or lower feed rates are applied to achieve undamaged surfaces. Figure 10 shows the pressure distribution along the grinding wheel axial direction. For the flat nozzle the pressure is slightly higher at a volume flow of 18l/min versus 6l/min supplied by the four round nozzles. The round nozzles distribute the fluid evenly over the width of the workpiece respectively grinding wheel even if too little amount of fluid, as 2l/min, is provided. In Table 2 the mean values of the volume fraction, velocity and pressure are summarized for the two nozzle types and different flow rates.

Table 2. Mean values in grinding zone

Type	Q [l/min]	Volume Fraction [-]	Velocity [m/s]	Pressure [bar]
Four Round Nozzles	2	0.155	18.5	1.4
	4	0.995	41.4	7.0
	6	0.995	41.5	6.7
	18	0.995	42.8	7.4
Flat Nozzle	12	0.348	17.9	2.1
	18	0.991	39.5	7.5
	30	0.994	43.6	7.7

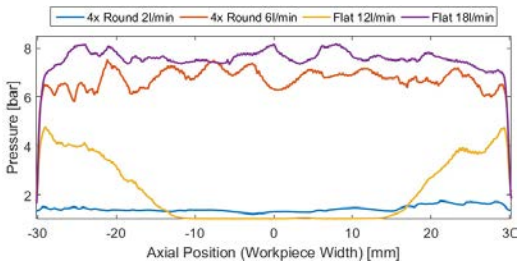

Fig. 10. Pressure distribution of coolant in grinding contact zone over workpiece width of different nozzles and flow rates.

4. Conclusions and outlook

A detailed and general analytical solution for the airflow of rotating grinding wheels is only possible with strong simplifications. The general profile and its dependencies are shown in the second chapter. Considering geometric constraints like non-cylindrical wheel geometry, one sided clamping and the protective casting of the grinding wheel CFD simulations become a possibility to investigate the flow profiles. In this work the effect of the air boundary layer of a rotating grinding wheel on coolant jets is investigated by using CFD simulations for two different nozzle designs. The set-up is chosen in accordance with real grinding tests and compared to the measured performance.

Numerical simulations of the jet flow interaction with the rotating grinding wheel are proving to be a utile tool for the design and optimization of nozzles regarding the minimization of the required volume flow of coolant. A uniform filling of the grinding gap with coolant is achieved by employing a nozzle with an exit orifice width of less than 10% of the grinding zone width and an exit velocity of the coolant of about 37% of the cutting speed. This demonstrates high possible savings and enhanced useful flow with optimized nozzle design.

Based on these studies further nozzle designs as well as nozzle positions (angle and distance) can be investigated and optimized. Parameter studies are proposed to estimate the maximum possible distance without quality reduction between two round nozzles along the grinding wheel profile in order to minimize the coolant volume flow and thus the energy consumption of the machine by employing a minimum number of real grinding tests.

Acknowledgements

The authors gratefully acknowledge the financial contribution of the Swiss Commission for Technology and Innovation (No. 13963.2 PFIW-IW) and Fritz Studer AG as well as Blaser Swisslube for providing machine, tools and coolant respectively. The authors thank also Jean-Paul Kunsch for valuable discussions.

References

[1] Malkin S, Anderson RB. Thermal Aspects of Grinding Part 1 - Energy Partition. *J. Of Engineering For Industry*; 1974, p. 1177-1183.

[2] Malkin S. Thermal Aspects of Grinding Part 2 - Surface Temperatures and Workpiece Burn. *J. of Engineering for Industry*; 1974, p. 1177-1183.

[3] Klocke F, Eisenblätter G. Dry Cutting. *Annals of the CIRP Annals* 46/2; 1997, p. 519-526.

[4] Engineer F, Guo C, Malkin S. Experimental Measurement of Fluid Flow Through the Grinding Zone. *J. of Engineering for Industry*; 1992, Vol. 114, p. 61-66.

[5] Gviniashvili VK, Woolley NH, Rowe WB. Useful coolant flowrate in grinding. *International Journal of Machine Tools & Manufacture* 44; 2004, p. 629–636.

[6] Ebbrell S, Woolley NH, Tridimas YD, Allanson DR, Rowe WB. The effects of cutting fluid application methods on the grinding process. Int. J. of Machine Tools & Manufacture 40; 2000, p. 209–223.

[7] Wittmann M, Heinzel C, Brinksmeier E. Evaluating the Efficiency of Coolant Supply Systems in Grinding. *Production Engineering* Vol. XI/2; 2004, p. 39-42.

[8] Baumgart C, Callejo Goena N, Kuster F, Wegener K. Optimierung der Kühlschmiermittelverteilung vor dem Schleifspalt beim Aussenrundschleifen; 2016, *1. Schweizer Schleif-Symposium*, Zürich, Schweiz.

[9] Baumgart C, Scheer ABM, Kuster F. Auslegung und Gestaltung der KSS-Zuführung beim Aussenrundschleifen; 2016, *11. Seminar Moderne Schleiftechnologie und Feinstbearbeitung*, Stuttgart, Deutschland.

[10] Davies TP, Jackson RG. Air flow around grinding wheels. *Precision Engineering*; 1981, p. 225-228.

[11] Shibata J, Goto T, Yamarnoto M. Characteristics of Air Flow Around a Grinding Wheel and Their Availability for Assessing the Wheel Wear. *CIRP Annals* 31/1; 1982, p. 233-238.

[12] Wu H, Morgan MN, Lin B. An experimental investigation of air boundary layer flow in grinding using the laser doppler anemometry technique. *Int. J. Abrasive Technology*, Vol. 4/2; 2011.

[13] Wang C, Zhang L, Yang C. Analysis and Simulation of Air Flow Field Surrounding Grinding Wheel. *Advanced Materials Research* Vol. 1027; 2014, p. 12-15.

[14] Hosokawa A, Tokunaga K, Ueda T, Kiwata T, Koyano T. Drastic reduction of grinding fluid flow in cylindrical plunge grinding by means of contact-type flexible brush-nozzle. *CIRP Annals* 65; 2016, p. 317–320.

[15] Webster JA, Cui C, Mindek Jr. RB. Grinding Fluid Application System Design. *CIRP Annals* 44; 1995, p. 333-338.

[16] Schlichting H, Gersten K. Grenzschicht-Theorie. *Springer-Verlag Berlin Heidelberg* 10th ed.; 2006, p.120-125.

[17] Li C, Han Z. Modelling and simulation of the airflow field in wedge-shaped zone during the high-speed grinding. *Int. J. Abrasive Technology*, Vol. 6/2; 2013, p. 114-131.